J Mater Sci (2009) 44:6408–6415
DOI 10.1007/s10853-009-3884-y

Synthesis and chemical properties of photoluminescent self-doped polyanilines

Isao Yamaguchi · Hideo Higashi · Moriyuki Sato

Received: 8 August 2009 / Accepted: 11 September 2009 / Published online: 24 September 2009

Abstract Fluorescent self-doped polyanilines (PAS-AntPy-a and PAS-AntPy-b) were obtained by the pyridinium sulfonation of poly(2-methoxyaniline-5-sulfonic acid) (PAS) with 4-(2-anthracene-9-yl-vinyl)pyridine (AntPy). The degrees of pyridinium sulfonation in PAS-AntPy-a and PAS-AntPy-b were 0.70 and 0.97, respectively. A neutral polyaniline with an AntPy side unit (PANI-AntPy) was synthesized by the oxidative polymerization of *N*-(2-aminophenyl)-4-(2-anthracene-9-yl-vinyl)pyridinium chloride. The UV-vis spectra of PAS-AntPy-a and PAS-AntPy-b exhibited an absorption due to the polaron band that was derived from the protonation of amine groups in the polyaniline backbone with the remaining sulfonic acid proton. In contrast, PANI-AntPy did not exhibit absorption due to the polaron band. PAS-AntPy-a, PAS-AntPy-b, and PANI-AntPy were photoluminescent in a solution. The electric conductivity of PAS-AntPy-a was $\sigma = 1.5 \times 10^{-7}$ S cm^{-1}, which was higher than that of H_2SO_4 doped PANI (4.2×10^{-9} S cm^{-1}) reported previously.

Introduction

Polyaniline (PANI), one of the most well-known conductive polymers, has been extensively studied due to its interesting chemical properties and practical applications [1–3]. Sulfonated polyanilines (SPAN) have attracted much attention because of their self-doping properties, improved processability, and potential industrial applications [4–11]. The sulfonic acid proton in SPAN is considered to play an important role in self-doping. It has been substituted with alkaline metals and functional groups to bring about additional functionalities on SPAN. For example, the use of alkaline metal salts of SPAN as solid polymer electrolytes for batteries has been investigated [4]. Recently, we reported the self-doping behavior in 4,4′-bipyridinium salts of SPAN that maintained a conductive state over a wide pH range [12].

Photoluminescent conducting polymers have attracted much attention because of their potential applications in biosensors [13–17] and EL devices [18, 19]. PANIs with fluorescent side groups have been synthesized by the direct incorporation of emitting molecules onto a polyaniline backbone as pendant groups [20]. Photoluminescent conducting PANIs can be useful as an electron mediator in biosensors. However, to the best of our knowledge, there have been no reports on such PANIs. Thus, investigation of the chemical properties of the photoluminescent conducting PANIs will afford fundamental information for the development of new functional materials. In this study, to develop PANI-based photoluminescent conducting materials, we carried out the pyridinium sulfonation of poly (2-methoxyaniline-5-sulfonic acid) (PAS) with fluorescent 4-(2-anthracene-9-yl-vinyl)pyridine (AntPy). This simple reaction can be useful for the preparation of the proposed photoluminescent conducting PANI; the remaining sulfonic acid group in the pyridinium-sulfonated products (PAS-AntPy) can serve as a dopant to bring about electric conductivity. In this work, two PAS-AntPys with different degrees of pyridinium sulfonation were synthesized.

Herein, we report the results of the synthesis of PAS-AntPy and describe its optical and electrochemical properties; in addition, we report a comparison of the optical and electronic properties of PAS-AntPy with a neutral

I. Yamaguchi (✉) · H. Higashi · M. Sato
Faculty of Science and Engineering, Department of Material Science, Shimane University, 1060 Nishikawatsu, Matsue 690-8504, Japan
e-mail: iyamaguchi@riko.shimane-u.ac.jp

PANI with an AntPy side group and pyridinium and sodium salts of PAS.

Experimental section

Materials and measurements

Poly(2-methoxyaniline-5-sulfonic acid) (PAS) [4], *N*-(2,4-dinitrophenyl)-4-pyridylpyridinium chloride [21], and PAS-Na [4] were prepared according to the literatures. Other chemicals were purchased and used without further purification. Solvents were purified by distillation and stored under nitrogen atmosphere.

Microanalysis of C, H, and N was carried out with a Yanagimoto Type MT-5 CHN autocorder. IR and NMR spectra were recorded on a JASCO FT/IR-410 PLUS spectrophotometer and a JEOL AL-400 spectrometer, respectively. UV-vis and PL spectra were obtained on a JASCO V-560 spectrometer and a JASCO FP-6200, respectively. Powder X-ray diffraction analysis was performed with a Rigaku Rint 2200/AFC-7. Cyclic voltammetry (CV) of the polymers was conducted in a DMSO solution containing 0.10 M $[Et_4N]BF_4$ with a BAS 100B. Resistance of the polymers was measured by using a four-probe method with a HORIBA COND METER ES-51. The electric conductivity (σ) was calculated from a following scheme: $\sigma = (1/R) \cdot (\ln 2/\pi) \cdot (1/d)$, where R = resistance of the molded pellet of the polymers and d = thickness of the molded pellet. The pellet thickness was measured with a micrometer.

Synthesis of (9-anthrylmethyl)triphenylphosphonium chloride

9-Chloromethylanthracene (4.5 g, 20 mmol) and triphenylphosphine (5.3 g, 20 mmol) were dissolved in DMF (80 mL). After the reaction solution was stirred at 80 °C for 12 h, the precipitate from the reaction solution was collected by filtration. The precipitate was washed with DMF and diethyl ether and dried under vacuum to give AntPy as a yellow powder (9.2 g, 91%). ^{1}H NMR (400 MHz, $CDCl_3$): δ 8.31 (d, $J = 3.6$ Hz, 1H), 7.86 (d, $J = 8.8$ Hz, 4H), 7.51–7.62 (9H), 7.39–7.49 (6H), 7.24 (t, $J = 8.4$ Hz, 2H), 7.07 (t, $J = 6.8$ Hz, 2H), 6.34 (t, $J = 14.4$ Hz, 2H). ^{13}C NMR (100 MHz, $CDCl_3$): δ 134.2, 133.8, 130.4, 129.2, 128.3, 128.2, 125.7, 124.4, 123.5, 118.2, 117.7, 116.9, 24.6. Calcd for $C_{33}H_{26}ClP$: C, 81.06; H, 5.36. Found: C, 81.22; H, 5.60.

Synthesis of AntPy

To a methanol solution of (9-anthrylmethyl)triphenylphosphonium chloride (1.0 g, 2.0 mmol) was added 4-pyridinecarboxaldehyde (0.26 g, 2.4 mmol) and sodium methoxide (0.14 g, 2.6 mmol). After the reaction solution was refluxed for 8 h, the solvent was removed under vacuum. The resulting solid was washed with cold methanol and water and dried under vacuum to give AntPy as a light yellow powder (0.37 g, 65%). ^{1}H NMR (400 MHz, $CDCl_3$): δ 8.68 (d, $J = 6.0$ Hz, 2H), 8.45 (s, 1H), 8.28 (m, 2H), 8.16 (d, $J = 16.8$ Hz, 1H), 8.03 (m, 2H), 7.53 (d, $J = 6.4$ Hz, 2H), 7.50 ($J = 6.8$ Hz, 2H), 7.49 ($J = 6.4$ Hz, 2H), 6.91 (d, $J = 16.4$ Hz, 1H). ^{13}C NMR (100 MHz, $CDCl_3$): δ 150.4, 144.3, 134.7, 131.3, 131.2, 129.7, 129.5, 128.8, 127.2, 125.8, 125.4, 125.2, 120.9. Calcd for $C_{21}H_{15}N$: C, 89.65; H, 5.37; N, 4.98. Found: C, 89.49; H, 5.20; N, 4.88.

Synthesis of PAS-AntPy-b

After the DMSO (5 mL) solution of PAS (0.10 g, 0.50 mmol) and AntPy (0.21 g, 0.75 mmol) was stirred at 60 °C for 24 h, the solvent was removed under vacuum. The resulting solid was washed with water and acetone and dried under vacuum to give PAS-AntPy-b as a black powder (0.11 g, 45%). ^{1}H NMR (400 MHz, DMSO-d_6): δ 8.82 (2.91H), 8.59 (0.97H), 8.30 (3.88H), 8.07 (1.94H), 7.51 (3.88H), 7.21 (d, $J = 14.8$ Hz, 1H), 7.16 (1H), 7.03 (1H), 6.91 (1H), 3.00 (3H). Calcd for $[(C_{112}H_{86}N_8O_{16}S_4)_{0.97}(C_{28}H_{26}N_4O_{16}S_4)_{0.03}]_n$: C, 69.41; H, 4.48; N, 5.83. Found: C, 69.49; H, 4.16; N, 5.37.

PAS-AntPy-a was synthesized by the reaction PAS and AntPy in a 1:1 molar ratio using the similar procedure as PAS-AntPy-b. Yield = 51%. ^{1}H NMR (400 MHz, DMSO-d_6): δ 8.82 (2.1H), 8.59 (0.7H), 8.30 (2.8H), 8.07 (1.4H), 7.51(2.8H), 7.21 (d, $J = 14.8$ Hz, 1H), 7.16 (1H), 7.03 (1H), 6.91 (1H), 3.00 (3H). Calcd for $[(C_{112}H_{86}N_8O_{16}S_4)_{0.70}(C_{28}H_{26}N_4O_{16}S_4)_{0.30}]_n$: C, 65.54; H, 4.31; N, 5.99. Found: C, 65.52; H, 4.02; N, 5.51.

Synthesis of AntPy-DNB

The acetone solution (2 mL) of AntPy (0.24 g, 0.85 mmol) and 1-chloro-2,4-dinitrobenzene (0.17 g, 0.86 mmol) was refluxed for 4 h. The precipitate from the reaction solution was collected by filtration, washed with acetone, and dried under vacuum to give AntPy-DNB as a light yellow powder (0.17 g, 40%). ^{1}H NMR (400 MHz, DMSO-d_6): δ 9.35 (d, $J = 6.8$ Hz, 2H), 9.22 (d, $J = 16.4$ Hz, 1H), 9.16 (d, $J = 2.4$ Hz, 1H), 9.00 (dd, $J = 2.4$ and 8.8 Hz, 1H), 8.78 (d, $J = 6.8$ Hz, 2H), 8.76 (s, 1H), 8.46 (d, $J = 5.6$ Hz, 2H), 8.43 (d, $J = 6.0$ Hz, 1H), 8.20 (d, $J = 7.6$ Hz, 2H), 7.56 (m, 4H), 7.53 (d, $J = 16.4$ Hz, 1H). ^{13}C NMR (100 MHz, $CDCl_3$): δ 155.0, 149.0, 145.4, 143.2, 140.4, 138.7, 132.1, 132.0, 130.9, 130.2, 129.7, 129.2, 129.1, 129.0, 127.0, 126.0, 125.7, 125.3, 124.1, 121.5. Calcd for

$C_{27}H_{18}ClN_3O_4 \cdot 0.5H_2O$: C, 65.79; H, 3.89; N, 8.52. Found: C, 65.71; H, 4.00; N, 8.49.

Synthesis of AntPy-PA

After the ethanol solution (5 mL) of AntPy-DNB (0.31 g, 0.65 mmol) and 1,2-diaminobenzene (0.14 g, 1.3 mmol) was refluxed for 12 h, the solvent was removed under vacuum. The resulting solid was washed with acetone and dried under vacuum to give AntPy-PA as a red powder (0.14 g, 54%). ^{1}H NMR (400 MHz, DMSO-d_6): δ 9.21 (d, $J = 15.6$ Hz, 1H), 9.20 (d, $J = 6.8$ Hz, 2H), 8.83 (s, 1H), 8.80 (d, $J = 6.8$ Hz, 2H), 8.48 (d, $J = 8.4$ Hz, 2H), 8.29 (d, $J = 7.2$ Hz, 2H), 7.69–7.75 (m, 4H), 7.57 (d, $J = 16.8$ Hz, 1H), 7.48 (d, $J = 8.0$ Hz, 1H), 7.40 (d, $J = 8.0$ Hz, 1H), 7.08 (d, $J = 8.0$ Hz, 1H), 6.89 (t, $J = 8.0$ Hz, 1H), 5.78 (s, 2H). ^{13}C NMR (100 MHz, DMSO-d_6): δ 152.4, 149.0, 145.8, 138.4, 132.1, 130.9, 130.7, 130.1, 129.8, 129.1, 128.9, 128.5, 127.1, 127.7, 125.7, 125.3, 124.3, 119.4, 115.9. Calcd for $C_{27}H_{21}ClN_2 \cdot 0.2H_2O$: C, 78.61; H, 5.23; N, 6.79. Found: C, 78.70; H, 5/47; N, 6.55.

Synthesis of PANI-AntPy

AntPy-PA (0.082 g, 0.20 mmol) was dissolved in 1 M DMSO solution (4 mL) of HCl, and $(NH_4)_2S_2O_8$ (0.048 g, 0.20 mmol) was added to the solution. After the reaction solution was stirred at 20 °C for 24 h, the solvent was removed under vacuum. The resulting solid was washed with methanol and 0.05 M NaOH(aq) and dried under vacuum to give PANI-AntPy as a brown powder (0.013 g, 16%). ^{1}H NMR (400 MHz, DMSO-d_6): δ 9.16 (3H), 8.71 (3H), 8.36 (2H), 8.18 (2H), 7.56 (8H), 5.65 (0.19H). Calcd for $(C_{112}H_{74}N_8Cl_4)_{10}C_{26}H_{20}N_2 \cdot 1H_2O$: C, 80.46; H, 4.48; N, 6.71. Found: C, 80.89; H, 4.43; N, 7.08.

Synthesis of PAS-Py

To a DMSO solution (5 mL) of PAS (0.10 g, 0.50 mmol) was added pyridine (0.21 g, 0.75 mmol). After the reaction solution was stirred at 60 °C for 24 h, the solvent was removed under vacuum. The resulting solid was washed with methanol and dried under vacuum to give PAS-Py as a black powder (0.11 g, 51%). ^{1}H NMR (400 MHz, DMSO-d_6): δ 8.67 (1.9H), 8.04 (1H), 7.59 (1.9H), 7.23 (1H), 7.10 (1H), 6.98 (1H), 3.71 (3H). Calcd for $[(C_{48}H_{42}N_8O_{16}S_4)_{0.95}(C_{28}H_{26}N_4O_{16}S_4)_{0.05} \cdot 1.7H_2O]_n$: C, 49.95; H, 3.98; N, 9.67. Found: C, 49.97; H, 4.43; N, 9.08.

Results and discussion

Synthesis and characterization

4-(2-Anthracene-9-yl-vinyl)pyridine (AntPy) was synthesized by the Wittig reaction of (9-anthrylmethyl)triphenylphosphonium chloride and 4-pyridinecarboxaldehyde. The reaction of PAS with AntPy in 1:1 and 1:1.5 molar ratios resulted in the formation of PAS-AntPy-a and PAS-AntPy-b in 51 and 45% yields, respectively (Scheme 1). The ^{1}H NMR peak integral ratio of the protons in the polyaniline backbone to those in the pyridinium rings suggested that the degrees of pyridinium sulfonation (content of unit A) in PAS-AntPy-a and PAS-AntPy-b were 0.70 and 0.97, respectively. Elemental analysis also supported these structures.

To obtain a neutral polyaniline with AntPy side groups, a new aniline derivative AntPy-AP was synthesized by the 1:1 reaction of a Zincke salt (AntPy-DNB), which was obtained by the reaction of AntPy with 1-chloro-2,4-dinitrobenzene, with 1,2-diaminobenzene (Scheme 2a). The oxidative polymerization of AntPy-AP with ammonium

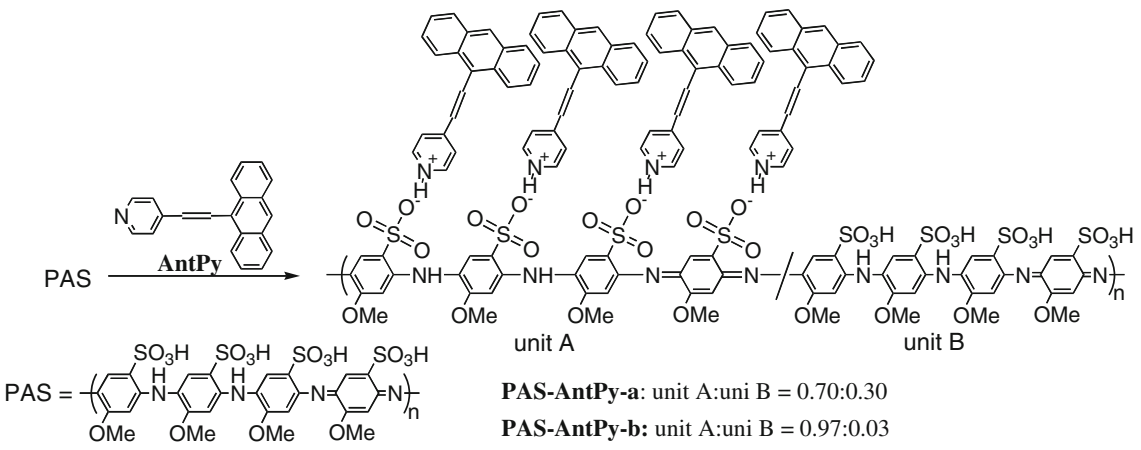

Scheme 1 Synthesis of PAS-AntPys

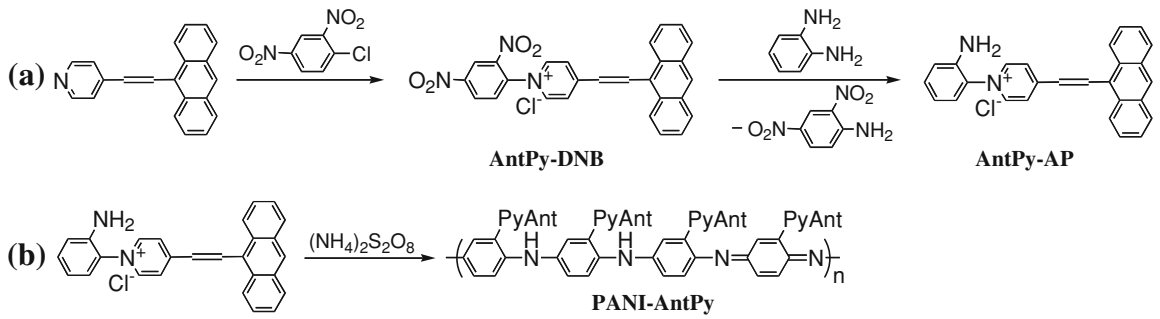

Scheme 2 Synthesis of AntPy-AP and PANI-AntPy

Scheme 3 Synthesis of pyridinium and sodium salts of PAS

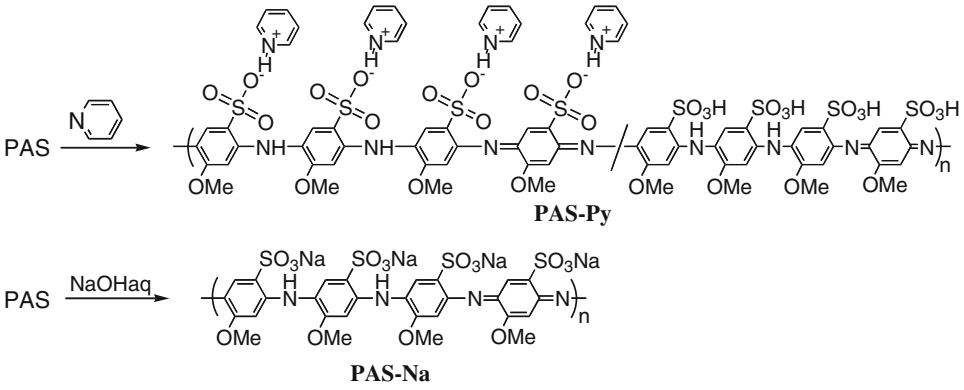

peroxodisulfate resulted in the formation of polyaniline with AntPy side groups (PANI-AntPy) in 16% yield (Scheme 2b). The low yield of PANI-AntPy was apparently due to the formation of low-molecular-weight products that were removed by the purification procedure.

To compare the chemical properties of PAS-AntPy-a, PAS-AntPy-b, and PANI-AntPy, pyridinium and sodium salts of PAS (PAS-Py and PAS-Na) were synthesized (Scheme 3). The degree of pyridinium sulfonation was determined to be 0.95 from the ^{1}H NMR peak integral ratio of the protons in the polyaniline backbone to those in the pyridinium rings. Elemental analysis suggested that sodium sulfonation proceeded completely.

PAS-AntPy-a, PAS-AntPy-b, PA-AntPy, PAS-Py, and PAS-Na were soluble in polar organic solvents such as *N*,*N*-dimethylformamide (DMF), dimethyl sulfoxide (DMSO), and *N*-methyl-2-pyrrolidone (NMP). As shown in Fig. 1, the η_{sp}/c values of PAS and PAS-PyAnt-b in DMSO at 30 °C increased as the concentration c decreased. This result suggests that the polymers behave as polymeric electrolytes in dilute solutions [22]. The viscosities of the solutions of PAS-PyAnt-b were higher than those of PAS, suggesting that PAS-PyAnt-b had a more extended structure than PAS in DMSO. DMSO solutions of PAS-PyAnt-a exhibited viscosities similar to those of PAS-PyAnt-b.

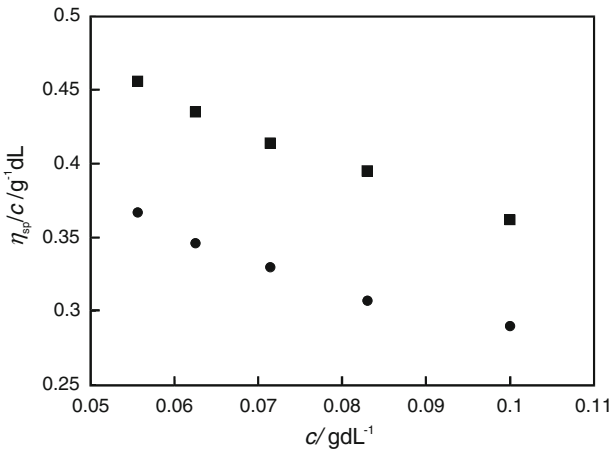

Fig. 1 η_{sp}/c vs c plots for PAS (*filled circle*) and PAS-AntPy-b (*filled square*) in DMSO at 30 °C

^{1}H NMR and IR spectra

Figure 2 shows the ^{1}H NMR spectra of AntPy and PAS-AntPy-a in DMSO-d_6. The peak assignments are shown in the figure. Peaks due to protons of the pyridinium ring ($H^{a'}$ and $H^{b'}$) and vinylene group ($H^{c'}$ and $H^{d'}$) in the ^{1}H NMR spectrum of PAS-AntPy-a were observed at lower

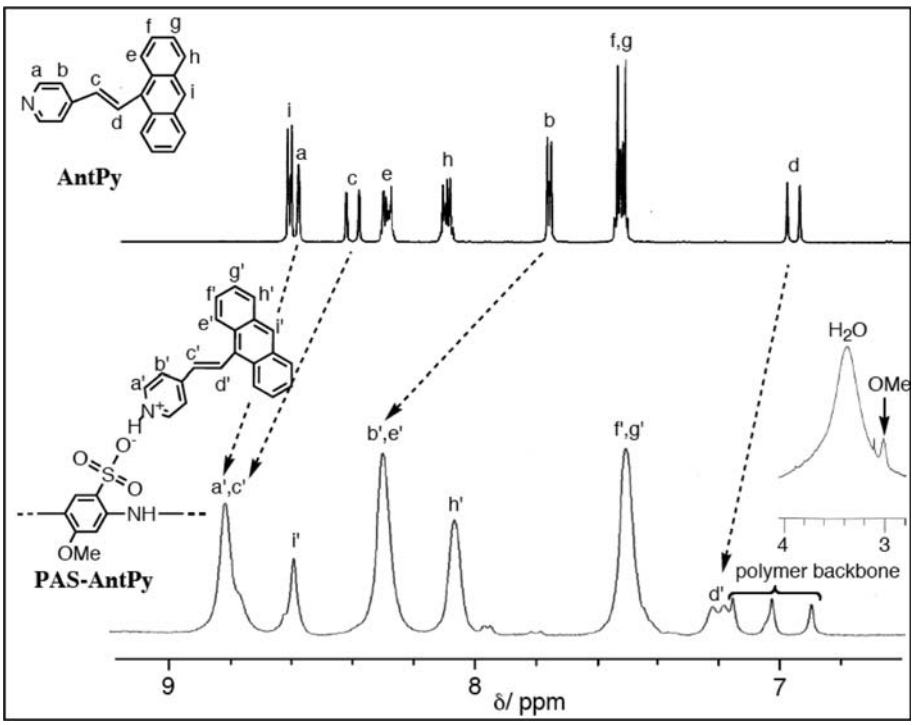

Fig. 2 ^{1}H NMR spectra of AntPy and PAS-AntPy-a in DMSO-d_6

magnetic field positions as compared to those in PyAnt because the pyridinium group of PAS-AntPy-a was bonded to the electron-withdrawing sulfo group. However, peaks due to the anthryl protons ($H^{e'} \sim H^{i'}$) in PAS-AntPy-a were observed at almost the same positions as those in PyAnt. The peaks at δ 6.91, 7.03, and 7.16 were assigned to the protons of the polyaniline backbone. The coupling constant between the vinylene protons was $J^{c\,d}_{H\text{-}H} = 16.8$ Hz, suggesting that the vinylene group has a trans geometrical structure. Figure 3 shows the ^{1}H NMR spectra of AntPy-AP and PANI-AntPy in DMSO-d_6. Peak assignments are shown in the figure. PANI-AntPy exhibited broad peaks; however, the peak positions were similar to those of AntPy-AP. These observations suggested that the 2-animophenyl ring in AntPy-AP and the polyaniline backbone in PANI-AntPy have a similar electronic effect on the AntPy group. The peak at δ 5.65 in the ^{1}H NMR spectrum of PANI-AntPy was assigned to the terminal NH_2

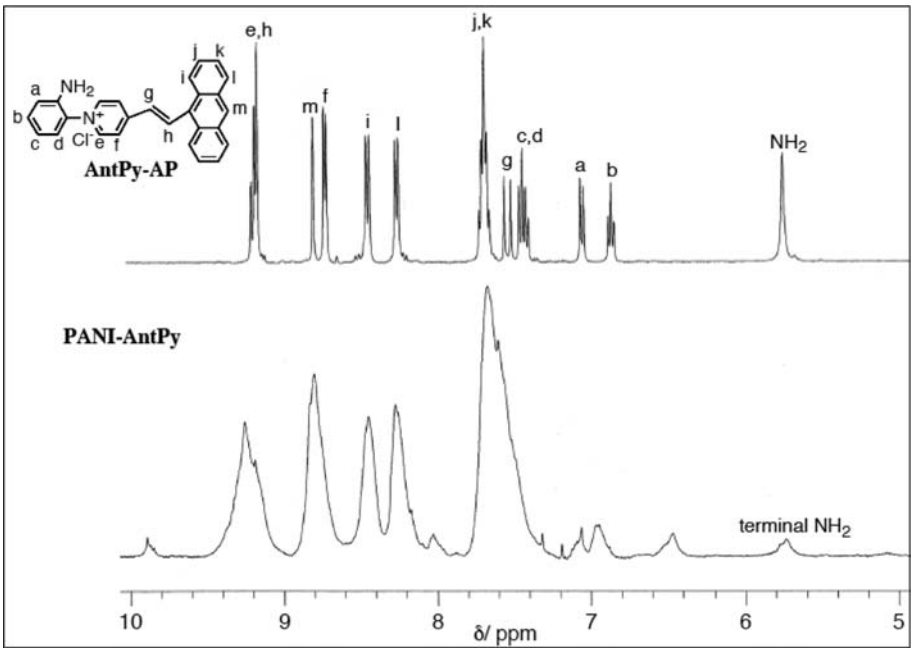

Fig. 3 ^{1}H NMR spectra of AntPy-AP and PANI-AntPy in DMSO-d_6

protons. The degree of polymerization (n) of PANI-AntPy was estimated to be 10 from the peak integral ratio of the protons in the terminal NH_2 group to those in the polyaniline backbone.

PAS exhibited an IR absorption due to ν(O–H) of the sulfonic acid group at 3400 cm^{-1}. However, the absorption due to ν(O–H) of the sulfonic acid group was almost negligible in the IR spectra of PAS-Py, PAS-AntPy-a, and PAS-AntPy-b. This interference is consistent with the fact that most of sulfonic acid protons of PAS-Py, PAS-AntPy-a, and PAS-AntPy-b are replaced with pyridinium or AntPy groups, respectively.

UV-vis and photoluminescence spectra

Figure 4 shows the UV-vis spectra of PAS-AntPy-a, PAS-AntPy-b, PAS-Py, PAS-Na, and PANI-AntPy in DMSO. PAS-AntPy-a and PAS-AntPy-b exhibited absorptions due to π–π^* transitions of the anthryl group in the range of 330–420 nm. The absorption peak at 477 nm in the UV-vis spectra of PAS-Py, PAS-AntPy-a, and PAS-AntPy-b is assignable to the polaron band of the self-doped polymer backbone that is derived from the protonation of the amine group with the sulfonic acid proton. This absorption wavelength is similar to that of PAS [4]. PAS-AntPy-b had a higher content of unit A than PAS-AntPy-a; however, the peak absorbance due to the polaron band is almost the same in each UV-vis spectra. This result is attributed to the assumption that the self-doping of the polyaniline backbone with the sulfonic acid proton in PAS-AntPy-a and PAS-AntPy-b is independent of the content of the remaining sulfonic acid group in the polymers. In contrast, the absorption peak due to the polaron band was not observed in the UV-vis spectrum of PAS-Na because the self-doping of the polymer backbone is inhibited by the presence of Na^+ instead of the sulfonic acid proton. PANI-AntPy exhibited shoulder absorptions due to π–π^* transitions of the AntPy group and benzonoid unit of the polyaniline backbone in the range of 360–410 nm. A broad absorption in the range of 560–700 nm was assigned to the quinoid unit of the polyaniline backbone. It has been reported that PANI with a 4,4′-bipyridinum group exhibits an absorption due to the polaron band at 474 nm derived from the electron transfer from the polymer backbone to the 4,4′-bipyridinum group [12]. However, PANI-AntPy did not exhibit an absorption due to the polaron band of the polymer backbone, suggesting that there was no electron transfer from the polymer backbone to the pyridinium group. From these results, the observation of the peak due to the polaron band in the UV-vis spectra of PAS-AntPy-a and PAS-AntPy-b is attributed to self-doping based on the protonation of amine groups in the polyaniline backbone with the sulfonic acid proton.

Figure 5 shows photoluminescence (PL) spectra of AntPy, PAS-AntPy-b, and PANI-AntPy in DMSO. The PL peak positions of AntPy, PAS-AntPy-b, and PANI-AntPy were 492, 507, and 509 nm, respectively. The longer PL peak positions of PAS-AntPy-b and PANI-AntPy as compared to that of AntPy are apparently due to the presence of the protonated pyridinium ring in PAS-AntPy-b and the conjugation of the AntPy group with the polymer backbone in PANI-AntPy, respectively. It has been reported that the PL peak position of the polymer-containing pyridine ring shifted to a longer wavelength after the protonation of the pyridine ring with acid [23]. PAS-Py did not exhibit PL.

Powder X-ray diffraction

Figure 6 shows powder X-ray diffraction patterns of PAS, PAS-Py, and PAS-AntPy-b. It has been reported that the reflection at $2\theta = 17.5°$ ($d = 5.12$ Å) in the XRD pattern of PAS is assigned to the $c/2$ axial repeat (namely, 002 spacing) [4]. The idealized molecular structures shown in Fig. 6 have a glide plane symmetry (mirror plane combined

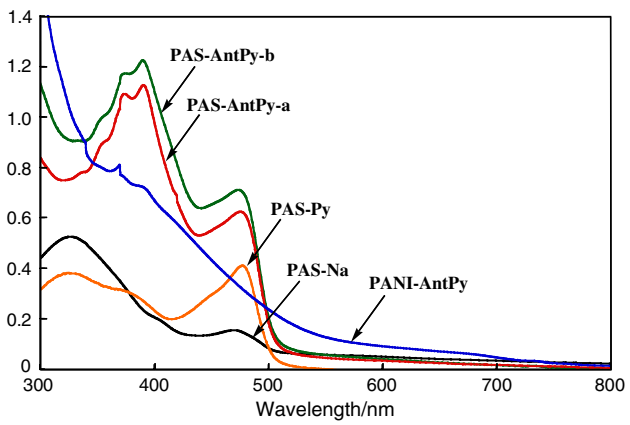

Fig. 4 UV-vis spectra of PAS-AntPy-a, PAS-AntPy-b, PAS-Py, PAS-Na, and PANI-AntPy in DMSO

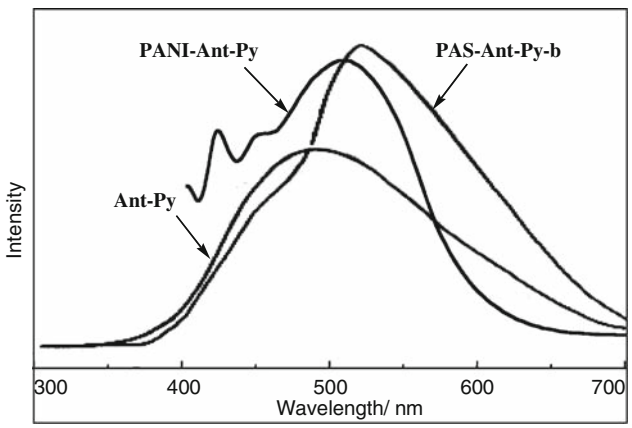

Fig. 5 Photoluminescence (PL) spectra of AntPy, PAS-AntPy-b, and PANI-AntPy in DMSO

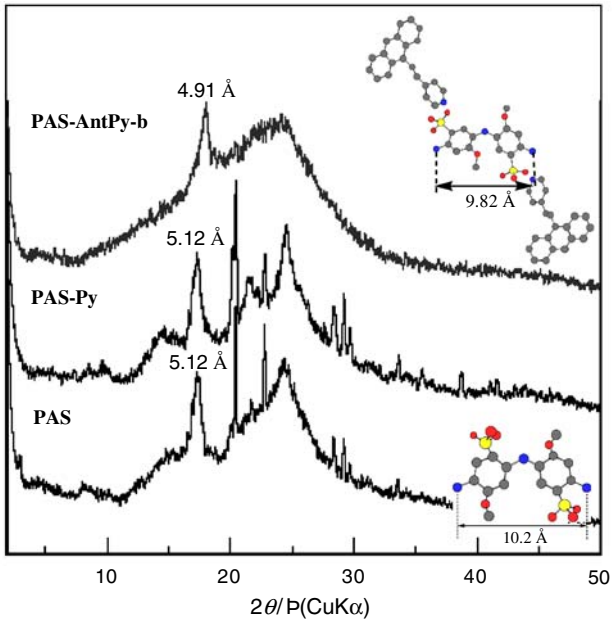

Fig. 6 X-ray diffraction patterns of PAS, PAS-Py, and PAS-AntPy-b

with the translation of $c/2$ along the chain axis), which arises from the rotation of the aromatic ring about their para axis. The $c/2$ axial repeat of PAS-Py ($d = 5.12$ Å) is the same as that of PAS, whereas that of PAS-AntPy-b ($d = 4.91$ Å) is shorter than that of PAS, which is apparently due to the vented structure of PAS-AntPy-b induced by the steric repulsion of the bulky anthryl groups between the repeating units.

Electric properties

Figure 7 shows cyclic voltammograms of PAS-AntPy-b and PANI-AntPy in a DMSO solution of $[Et_4N]BF_4$. The cyclic voltammogram of PAS-AntPy-b exhibited a broad anodic peak around 0.7 V due to the electrochemical oxidation of the polyaniline backbone. However, PANI-AntPy did not exhibit any peak due to electrochemical oxidation. This result is apparently due to difficulty in the electrochemical oxidation of PANI-AntPy because of the ring twisting along the polymer backbone generated from the steric hindrance of the bulky AntPy group. PAS-AntPy-b and PANI-AntPy exhibited a cathodic peak at the same potential (–1.00 V) due to the electrochemical reduction of the pyridinium ring and the corresponding oxidation (*n*-dedoping) peak was observed at –0.86 V.

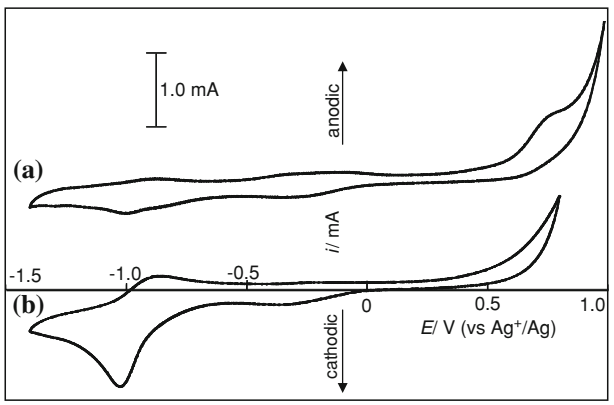

Fig. 7 Cyclic voltammograms of PAS-AntPy-b (**a**) and PANI-AntPy (**b**) in a DMSO solution of $[Et_4N]BF_4$

The electric conductivity of PAS-AntPy-a ($\sigma = 7.5 \times 10^{-6}$ S cm^{-1}) as determined by a four-probe method was higher than that of PAS-Py ($\sigma = 1.5 \times 10^{-7}$ S cm^{-1}). The higher σ value of PAS-AntPy-a is attributed to the occurrence of self-doping in PAS-AntPy-a. However, the σ value of PAS-AntPy-a was considerably lower than that of PAS ($\sigma = 4 \times 10^{-2}$ S cm^{-1} [4]). This result is because of the low content of the remaining sulfonic acid group as a dopant in PAS-PyAnt-a and because of ring twisting along the polymer backbone that is induced by the steric hindrance of the bulky AntPy group.

Conclusions

Photoluminescent conducting polyanilines (PAS-AntPy-a and PAS-AntPy-b) were obtained by the pyridinium sulfonation of poly(2-methoxyaniline-5-sulfonic acid) (PAS) with 4-(2-anthracene-9-yl-vinyl)pyridine (AntPy). The degree of pyridinium sulfonation was controlled by the feed molar ratio. The observation of absorption due to the polaron band in the UV-vis spectra of PAS-AntPy-a and PAS-AntPy-b suggested the occurrence of self-doping in the polymers. Because of self-doping, the electric conductivity of PAS-AntPy-a (1.5×10^{-7} S cm^{-1}) was higher than that of H_2SO_4 doped PANI (4.2×10^{-9} S cm^{-1}) reported previously. PAS-AntPy-a, PAS-AntPy-b, and PANI-AntPy were photoluminescent in a solution.

References

1. Trivedi DC (1997) In: Nalwa H (ed) Handbook of organic conductive molecules and polymers. Wiley, London, p 506
2. Kang ET, Neoh KG, Tan KL (1998) Prog Polym Sci 23:277
3. Gospodinova N, Terlemezyan L (1998) Prog Polym Sci 23:1443
4. Yamamoto T, Ushiro A, Yamaguchi I, Sasaki S (2003) Macromolecules 36:7075
5. Brenneman KR, Hsu CH, Shih H, Epstein AJ (2001) Macromolecules 34:2648
6. Shimizu S, Saitoh T, Uzawa M, Yuasa M, Yano K, Maruyama T, Watanabe K (1997) Synth Met 85:1337
7. Wei XL, Wang YZ, Long SM, Bobeczko C, Epstein AJ (1996) J Am Chem Soc 118:2545
8. Chen SA, Hwang GW (1996) Macromolecules 29:3950

9. Chen SA, Hwang GW (1995) J Am Chem Soc 117:10055
10. Yue J, Gordon G, Epstein AJ (1992) Polymer 33:4410
11. Kaneko M, Kaneto K (1998) React Funct Polym 37:155
12. Yamaguchi I, Shigesue S, Sato M (2009) React Funct Polym 69:91
13. Liu B, Bazan GC (2004) J Am Chem Soc 126:1942
14. Nilsson KPR, Inganäs O (2003) Nat Mater 2:419
15. Ho HA, Béra-Abérem M, Leclerc M (2005) Chem Eur J 11:1718
16. Song X, Wang HL, Shi J, Park JW, Swanson BI (2002) Chem Mater 14:2342
17. Liu B, Bazan GC (2004) Chem Mater 16:4467
18. Shirota Y, Kageyama H (2007) Chem Rev 107:953
19. Akcelrud L (2003) Prog Polym Sci 28:875
20. Amrithesh M, Aravind S, Jayalekshmi S, Jayasree RS (2008) J Alloys Compd 458:532
21. Yamaguchi I, Higashi H, Shigesue S, Shingai S, Sato M (2007) Tetrahedron Lett 48:7778
22. Fuoss RM, Strauss UP (1948) J Polym Sci 3246
23. Vaganova E, Meshulam G, Kotler Z, Rozenberg M, Yitzchaik S (2000) J Fluoresc 10:81